Preprint
UCRL-JC-151493

A comparison of PDE-based non-linear anisotropic diffusion techniques for image denoising

S. K. Weeratunga and C. Kamath

This article was submitted to
Image Processing: Algorithms and Systems II, SPIE Electronic Imaging, Santa Clara, January 2003.

December 23, 2002

U.S. Department of Energy

Lawrence
Livermore
National
Laboratory

A Comparison of PDE-based Non-linear Anistropic Diffusion Techniques for Image Denoising

Sisira K. Weeratunga and Chandrika Kamath

Lawrence Livermore National Laboratory, 7000 East Avenue, Livermore, CA 94551

ABSTRACT

PDE-based, non-linear diffusion techniques are an effective way to denoise images. In a previous study, we investigated the effects of different parameters in the implementation of isotropic, non-linear diffusion. Using synthetic and real images, we showed that for images corrupted with additive Gaussian noise, such methods are quite effective, leading to lower mean-squared-error values in comparison with spatial filters and wavelet-based approaches. In this paper, we extend this work to include anisotropic diffusion, where the diffusivity is a tensor valued function which can be adapted to local edge orientation. This allows smoothing along the edges, but not perpendicular to it. We consider several anisotropic diffusivity functions as well as approaches for discretizing the diffusion operator that minimize the mesh orientation effects. We investigate how these tensor-valued diffusivity functions compare in image quality, ease of use, and computational costs relative to simple spatial filters, the more complex bilateral filters, wavelet-based methods, and isotropic non-linear diffusion based techniques.

Keywords: Denoising, non-linear anisotropic diffusion, partial differential equations, bilateral filtering

1. INTRODUCTION

Denoising of image data has been an active area of research, with several different approaches being proposed using techniques such as wavelets, isotropic and anisotropic diffusion, bilateral filtering, etc. In a previous study,[1] we investigated the performance of different parameters in the definition and implementation of non-linear, isotropic diffusion for denoising images with additive Gaussian noise. In this earlier work, we followed the terminology used in the partial differential equation literature, where non-linear, isotropic diffusion was defined as the case where the diffusivity is a scalar function varying with the location in the image. In this paper, we consider the anisotropic case, where the diffusivity is a tensor, varying with both the location of a pixel in the image and the orientation of the local image geometry around the pixel. This allows us to smooth the image in the direction of an edge, but not perpendicular to it, thus maintaining the location and the strength of the edge. Note that our definition of anisotropic diffusion is different from that used in the image processing community,[2,3] where the term implies that the diffusivity is a scalar function varying with the location of a pixel in the image. We also compare and contrast the performance of anisotropic diffusion with the nonlinear isotropic diffusion, bilateral filters, wavelets, and spatial filters.

This paper is organized as follows. In Section 2, we introduce the idea behind the non-linear diffusion equation and discuss the isotropic and anisotropic variants. We describe various options that have been implemented for the anisotropic case. In Section 3, we consider the bilateral filter and its variants. Section 4 focuses on our numerical experiments on denoising using anisotropic diffusion and bilateral filtering. Using a synthetic test image and two real images from scientific domains, we also compare and contrast these techniques with spatial filters, isotropic diffusion, and wavelet-based thresholding schemes. Finally, in Section 5, we conclude with a brief summary of our work and ideas for future research.

Further author information: (Send correspondence to C.K.)
C.K.: Center for Applied Scientific Computing, L-561, P.O. Box 808, Lawrence Livermore National Laboratory, Livermore, CA 94551, U.S.A. E-mail: kamath2@llnl.gov

2. DENOISING USING ANISOTROPIC DIFFUSION

The idea behind the use of the diffusion equation in image processing arose from the use of the Gaussian filter in multi-scale image analysis. Convolving an image with a Gaussian filter K_σ:

$$K_\sigma(x,y) = \frac{1}{2\pi\sigma^2} exp\Big(-\frac{|x|^2+|y|^2}{2\sigma^2}\Big) \tag{1}$$

with standard deviation σ, is equivalent to the solution of the diffusion equation in two dimensions

$$\frac{\partial}{\partial t} I(x,y,t) = \nabla I(x,y,t) = \frac{\partial^2}{\partial x^2} I(x,y,t) + \frac{\partial^2}{\partial y^2} I(x,y,t) \tag{2}$$

where $I(x,y,t)$ is the two-dimensional image $I(x,y)$ at time $t = 0.5\sigma^2$, with initial conditions $I(x,y,0) = I_0(x,y)$, where I_0 is the original image. In a general form, this can be written as

$$\begin{aligned} \frac{\partial}{\partial t} I(x,y,t) &= \nabla \cdot \Big(c(x,y,t)\nabla I(x,y,t)\Big) \\ I(x,y,0) &= I_0(x,y) \end{aligned} \tag{3}$$

where $c(x,y,t)$ is the diffusion conductance or diffusivity of the equation, ∇ is the gradient operator, and $\nabla\cdot$ is the divergence operator. If c is a constant, independent of x, y, or t, it leads to a linear diffusion equation, with a homogeneous diffusivity. In this case, all locations in the image, including the edges are smoothed equally. This is, of course, undesirable, and a simple improvement would be to change c with the location x and y in the image, thus converting the equation into a linear diffusion equation with non-homogeneous diffusivity. If the function c is image dependent, then the linear diffusion equation becomes a non-linear diffusion equation. Such a formulation was proposed by Perona and Malik in their 1987 work.[2,3] By using a function c that was based on the derivative of the image at time t, they were able to control the diffusion near the edges in the image. Since then, several authors have enhanced this approach, and various options have been suggested for the diffusivity function, spatial discretization of the non-linear operator, and the numerical solution of the partial differential equation.[1]

In their work, Perona-Malik, as as several other authors, use the term "anisotropic" to refer to the case where the diffusivity is a scalar function varying with the location. However, in the partial differential equation community, this case is referred to as non-homogeneous non-linear isotropic diffusion. The term anisotropic is reserved for the case where the diffusivity is a tensor-valued function, varying with both the edge location and it's orientation. It is in the context of this latter terminology that we discuss our work in this paper.

As described earlier, non-homogeneous isotropic diffusion limits the smoothing of an image near pixels with a large gradient magnitude, which are essentially the edge pixels. As the diffusion near an edge is minimal, the noise reduction near the edge is also small. To address this, anisotropic diffusion was proposed to allow the diffusion to be different along different directions defined by the local geometry of the image.[4,5] Thus, diffusion across the edge can be prevented while allowing diffusion along the edge. This prevents the edge from being smoothed during the denoising.

The anisotropic form of the diffusion equation can be written as

$$\frac{\partial}{\partial t} I(x,y,t) = \nabla \cdot \Big(D(x,y,t)\nabla I(x,y,t)\Big), \tag{4}$$

where $D(x,y,t)$ is a symmetric positive-definite diffusion tensor. This 2×2 matrix can be written in terms of its eigenvectors $\mathbf{v}_1$ and $\mathbf{v}_2$, and eigenvalues λ_1 and λ_2, as follows

$$D \quad = \begin{bmatrix} \mathbf{v}_1 & \mathbf{v}_2 \end{bmatrix} \begin{bmatrix} \lambda_1 & 0 \\ 0 & \lambda_2 \end{bmatrix} \begin{bmatrix} \mathbf{v}_1^T \\ \mathbf{v}_2^T \end{bmatrix} \tag{5}$$

By appropriately choosing the eigenvalues and eigenvectors, different diffusivity tensors can be obtained. In this paper, we focus on edge-enhancing diffusion, where the eigenvectors are defined as follows:

$$\mathbf{v}_1 \parallel \nabla I_\sigma \tag{6}$$

and

$$\mathbf{v}_2 \perp \nabla I_\sigma. \tag{7}$$

Here, I_σ is the regularized (or smoothed) version of the image, that is, the image convolved with a Gaussian filter with standard deviation σ. Usually $\lambda_2 = 1$ to allow smoothing in the $\mathbf{v}_2$ direction. λ_1 can be chosen to be any of the diffusivity functions from the traditional non-homogeneous isotropic diffusion equation. This limits the diffusion in the direction of the gradient. In our work, we consider λ_1 to be defined using one of the following six diffusivity functions used in our earlier paper[1]:
Perona-Malik 1:

$$c(x,y,t) = 1/\Big(1 + \frac{|\nabla I_\sigma|^2}{K^2}\Big) \tag{8}$$

Perona-Malik 2:

$$c(x,y,t) = exp\Big(-|\nabla I_\sigma|^2/2K^2\Big) \tag{9}$$

Charbonnier:

$$c(x,y,t) = \Big(1 + \frac{|\nabla I_\sigma|^2}{K^2}\Big)^{-1/2} \tag{10}$$

Weickert (with m=2, 3, and 4):

$$c(x,y,t) = \begin{cases} 1 & \text{if } |\nabla I_\sigma| = 0 \\ 1 - exp\Big(-\frac{C_m}{(|\nabla I_\sigma|^2/K^2)^m}\Big) & \text{if } |\nabla I_\sigma| > 0 \end{cases} \tag{11}$$

where

$$1 = exp(-C_m)(1 + 2C_m m). \tag{12}$$

For $m = 2,\ 3,$ and 4, $C_m = 2.33666,\ 2.9183,$ and 3.31488. The conductance parameter K enables backward diffusion when it is smaller than the gradient ∇I_σ, thus enhancing the edges

2.1. Discretization of the anisotropic equation

The anisotropic diffusion equation (4) is solved using the finite difference method.[6] The spatial derivatives are approximated by central differences, while the temporal derivative is replaced by its forward difference approximation. This results in an explicit finite-difference equation of the form

$$\frac{I(k+1) - I(k)}{\Delta t} = A(I(k))\ I(k) \tag{13}$$

where $I(k)$ defines the image at time step k. $A(I(k))\ I(k)$ is a discretization of $\nabla \cdot (D\ \nabla I)$, which is essentially a convolution of the image with a mask with weights varying both spatially and temporally. The spatial discretizations used in our work results in 3×3 stencils and corresponds to the simpler standard discretization and the more complex non-negativity discretization.[7]

3. DENOISING USING THE BILATERAL FILTER

Recently, Tomasi and Manduchi[8] introduced a noniterative technique for removing noise from images. Although a simple technique, it has proven to be quite effective at removing noise. In addition, it has been shown[9,10] that the bilateral filter is related to isotropic diffusion (using the partial differential equation terminology). For these reasons, we consider it as one of the alternative techniques to compare the effectiveness of anisotropic diffusion.

The bilateral filter is simply a weighted average of the samples in a local neighborhood of a pixel. The weights are computed based on both the spatial proximity and the similarity of intensity values. The idea is to apply in the range of an image what traditional filters do in its domain. Since images typically vary slowly over space, the pixels near each other have similar values. In a traditional filter, which operates in the domain of an image, these pixel values are averaged together, with possibly some weighting that falls off with distance. As the noise in the nearby pixels is mutually less correlated than the signal values, the noise is averaged away, while the signal is preserved. A similar idea can be applied in the range of the image. Such a range filter would average pixel values with weights that decay with dissimilarity. In other words, the weights would be indicative of the intensity difference (in a gray-scale image) between the center pixel and its neighboring samples. Such a filter is non-linear as the weights depend on the image intensity.

In the bilateral filter, the weights of the range and domain filter are combined using simple multiplication of the weights at each point in the stencil. In our work, we follow Tomasi and Manduchi, and determine the weights using a Gaussian function. Specifically, the domain weights between pixels p_i and p_j are given by

$$w_d(p_i, p_j) = exp\Big(-\frac{1}{2}\Big(\frac{\parallel p_i - p_j \parallel}{\sigma_d}\Big)^2\Big) \tag{14}$$

where σ_d is the standard deviation in the domain and $\parallel p_i - p_j \parallel$ is the Euclidean distance between the pixels p_i and p_j. For the range weights between pixels p_i and p_j, we use

$$w_r(p_i, p_j) = exp\Big(-\frac{1}{2}\Big(\frac{\delta(I(p_i) - I(p_j))}{\sigma_r}\Big)^2\Big) \tag{15}$$

where σ_r is the standard deviation in the range and $\delta(I(p_i) - I(p_j))$ is a measure of the distance between the intensities at pixels p_i and p_j. If the two pixels vary widely in their intensities, as is the case at an edge, then the corresponding weight in the range filter is small, thus reducing the smoothing. For both these weights, a suitable filter support must be chosen; this is also the support of the bilateral filter. Each weight in the filter is the normalized product of the corresponding weights w_d and w_r. The bilateral filter thus has three parameters: σ_r, σ_d, and the filter support.

3.1. The Chen-Wang filter

Another idea similar to the bilateral filter has been proposed by Chen and Wang.[11] Here, the range filter is defined simply as

$$w_r(p_i, p_j) = \frac{1}{1 + |I(p_i) - I_\sigma(p_j)|} \tag{16}$$

where the second term in the denominator indicates the absolute value of the difference in pixel intensities between the pixel p_i and the pixel p_j in the original image that has been smoothed using a Gaussian with standard deviation σ. The pixel p_j is the center pixel in the filter. In other words, the weight at each pixel is related to how much that pixel differs from the smoothed version of the center pixel. The Chen-Wang filter is then the standard Gaussian filter on the domain, multiplied by the range filter above, with a suitable scaling so that the filter coefficients sum to 1.0. I_σ, which is the original image convolved with a Gaussian is referred to as the pre-filtered image. The original Chen-Wang filter thus has two parameters: σ and the filter support.

In the original Chen-Wang filter, the same Gaussian and filter support are used for the domain filter and for obtaining the pre-filtered image I_σ. However, if the image has small scale structure, this may get smoothed in the calculation of I_σ. So, we have modified the original version of the Chen-Wang filter to accomodate a different σ and filter support for the Gaussian used in the pre-filtering. This modified Chen-Wang filter thus has four parameters: the σ and filter support for the domain filter (the same filter support is used for the range filter) and the σ and filter support for the Gaussian used in the pre-filtering.

4. EXPERIMENTAL RESULTS

In this section, we describe the results of our experiments using non-linear anisotropic diffusion, the bilateral filter, and the Chen-Wang filter to denoise various scientific images. Using images which have been corrupted by

additive Gaussian noise, we explore the effectiveness of denoising as we change the various parameters described above. We also compare the results with our earlier work on non-homogeneous isotropic diffusion, wavelet-based denoising, and spatial filters.

4.1. Experimental images

In order to evaluate the different diffusion-based denoising methods, we have chosen three test images (see Figure 1). The first is a synthetic image chosen to enable experimentation with different parameters and to verify the accuracy of implementations. This is a rectangular image, and unlike most images that have dimensions that are power of 2, its size is 462 by 249. The other two images are from the scientific domain - one is an image of a lung taken from http://www-itg.lbl.gov/ImgLib.project/homepage.html and the other is an image of a galaxy from http://astro.u-strasbg.fr/ fmurtagh/multires/quick.html. In order to evaluate the effects of applying diffusion-based denoising, we have added Gaussian noise, with standard deviation of 20, to each of these images, as shown in Figure 1. Once the diffusion process is applied to the noisy image, its effectiveness in removing the noise is obtained by calculating the mean-squared error(MSE) relative to the original image as follows:

$$MSE = \frac{1}{NM} \sum_{i=1}^{N} \sum_{j=1}^{M} (I_{orig}(i,j) - I_{denoised}(i,j))^2, \tag{17}$$

where I_{orig} indicates the original uncorrupted image and $I_{denoised}$ is the image after denoising. The lower this number, the better the effect of the denoising. Note that this measure does not necessarily imply that an image with a lower MSE is also more visually pleasing. We could also have used other measures for evaluating the performance of the denoising techniques such as the one norm, or the normalized MSE.

In the results presented, the term "filter support" is used to indicate the half-width of the filter. The true size of the filter is therefore (2*filter_support +1).

4.2. Experiments with the bilateral filters

In this section, we discuss the results of our experiments with the two bilateral filters: the modified Chen-Wang filter and the Tomasi-Manduchi filter. For both filters, we tried different parameters to understand the sensitivity of the results to these parameters. The resulting reduction in noise using the modified Chen-Wang filter is reported in Tables 1, 2, and 3. The results are for a single iteration of the modified Chen-Wang filter. Using more than one iteration generally degraded the image. The corresponding results for the Tomasi-Manduchi filter are reported in Tables 4, 5, and 6. Again, the results are for a single iteration of the filter, as proposed in the Tomasi-Manduchi paper. However, it is possible to run multiple iterations of this filter as well.

4.3. Experiments with anisotropic diffusion

We next discuss the results of our experiments with the edge-enhancing anisotropic diffusion (Section 2) to denoise our three images. We varied several parameters including the diffusivity function applied parallel to the gradient, the conductance K that controls the diffusivity, and the spatial discretization. The total diffusion time was set to 1.0 and the time step determined by the stability restrictions on the explicit time-advancement method. For the regularization used in the calculation of the diffusivity, we set $\sigma = 1.0$. This regularization is done by solving the linear isotropic diffusion equation with explicit time advancement. Again, the diffusion time is calculated based on the value of σ. The resulting reduction in image noise is reported in Tables 7, 8, and 9.

4.4. Comparison of the various methods

In this paper, we have conducted a limited set of experiments on our test images. Further studies on other images, with different noise levels are required before we can make any conclusive statements about the performance of each of the methods. However, based on our experimental studies using the three test images with additive Gaussian noise, we can make some general observations. First, all the techniques we tried have several user-prescribed parameters that must be selected carefully for best results. In addition, the techniques are sensitive to small changes in these parameters. Since we have a "clean" original image, as well as one with added noise, we can use the reduction in the MSE to guide our choice of parameters. However, in the real world, we do not have

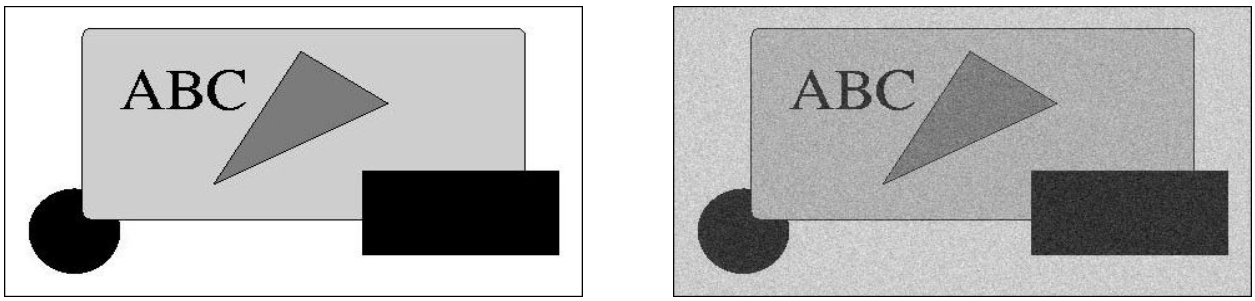

(a) (b)

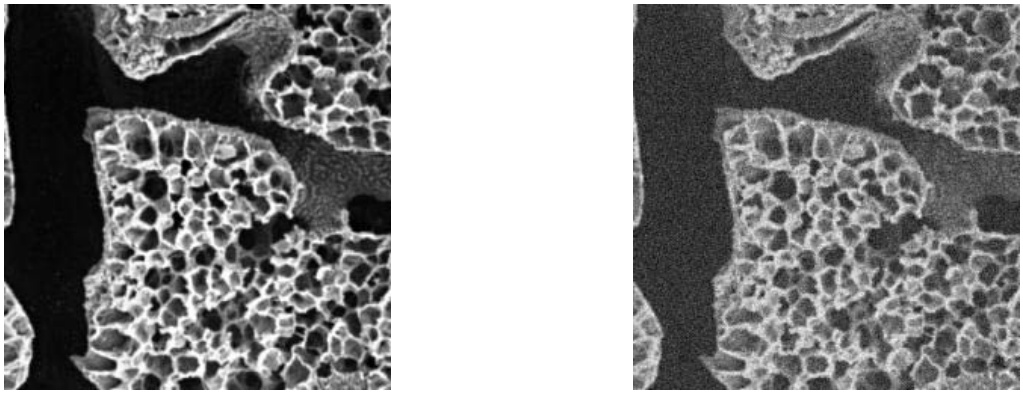

(c) (d)

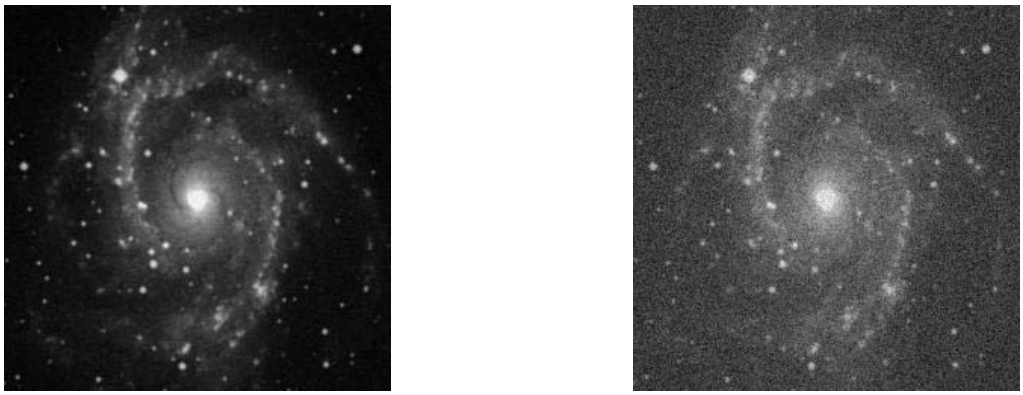

(e) (f)

Figure 1. Original images ((a), (c), and (e)) and the corresponding images with additive Gaussian noise of standard deviation 20 ((b), (d), and (f))

Table 1. Test image 1: Mean-squared error as a function of the four input parameters for the modified Chen-Wang filter. A pre-filter σ of 0.0 indicates that no pre-filtering is done. The MSE of the noisy image is 401.16.

Domain filter support	Domain filter σ	Pre-filter support	Pre-filter σ	MSE
4	2.0	2	0.5	215.7
3	2.0	2	0.5	210.2
2	2.0	2	0.5	196.1
2	1.0	2	0.5	169.0
2	0.5	2	0.5	239.6
2	1.0	1	0.5	168.7
2	1.0	1	0.25	320.1
2	1.0	1	0.75	250.1
2	1.0	1	1.0	299.2
2	1.0	1	1.5	337.2
2	1.0	1	0	323.5
4	1.0	1	0	322.4
4	2.0	1	0	227.4
4	3.0	1	0	195.4
4	4.0	1	0	185.0
4	10.0	1	0	176.2
5	1.0	1	0	322.4
5	2.0	1	0	225.2
5	3.0	1	0	189.6
6	5.0	1	0	173.9
7	5.0	1	0	174.1

a clean image, and therefore the parameter selection is guided by a visual examination of the denoised image, which may not be practical when we have to denoise several unrelated images.

For the modified Chen-Wang filter, we observe that having separate filter support and σ for the pre-filtering is helpful - however, turning off the pre-filtering completely (indicated by a pre-filter σ of 0.0 in the tables), may not be desirable. It is also not clear if a larger domain filter support is helpful in reducing the MSE.

The same observation can also be made for the Tomasi-Manduchi filter - a larger filter support leads to higher computational cost, without a corresponding reduction in the MSE. We also observe that the σ for the range filter has to be reasonably large. For the synthetic test image, the best result with the Tomasi-Manduchi filter (MSE = 28.7) far outperforms the best results with the other filters (modified Chen-Wang = 168.7, anisotropic = 71.9, isotropic = 41.41).

Comparing the results of the edge-enhancing anisotropic diffusion with our previous study of non-homogeneous isotropic diffusion, we observe several similarities. The Charbonnier diffusivity function is not as effective as the others. The denoising is sensitive to the value of the conductance parameter K. Also, the more complex non-negativity discretization performs better than the simpler standard discretization.

Figure 2 presents some of the best results for the different methods on the three test images. Panels (a) and (b) are the best results for the synthetic image using the Tomasi-Manduchi filter, and the anisotropic diffusion filter. Panels (c), (d), and (e) are the best results (with MSE = 157.4, 151.2, and 148.3) for the lung image for the three methods (modified Chen-Wang, Tomasi-Manduchi, and edge-enhancing anisotropic diffusion). Panels (f), (g), and (h) are the best results (with MSE = 57.7,64.6, and 39.0) for the galaxy image for the three methods.

For comparison, the best results in MSE using non-homogeneous isotropic diffusion for the synthetic image, the lung, image and the galaxy image, are 41.41, 140.1, and 39.52, respectively.[1] The best results using spatial filters (MMSE followed by a Gaussian, both with a filter size of 3) for the lung and galaxy images is 193.00 and 43.84, respectively. The best results using wavelet thresholding (Symmlet12 wavelet, with three levels of wavelet

decomposition, and periodic boundary conditions, using the SURE thresholding, applied at a pyramid level) for the lung and galaxy images is 158.43 and 52.33, respectively.

5. SUMMARY AND FUTURE WORK

In this paper, we presented a comparison of three image denoising methods that were published recently, namely a modified version of the Chen-Wang filter, the Tomasi-Manduchi bilateral filter, and the edge-enhancing anisotropic diffusion filter, where the diffusivity is a tensor-valued function varying with the location and orientation of edges in an image. This work is an extension of earlier work,[1] where-in we compared the non-linear isotropic diffusion filter with wavelet thresholding and spatial filters. Our early experiments with the new techniques indicate that they can be competitive. However, they do have several parameters that must be set appropriately for best performance. Since the result is quite sensitive to these parameters, this can be a difficult process.

In our future work, we plan to investigate the techniques further by conducting additional experiments on other images with different noise types and levels. We also plan to carry out a systematic investigation of the sensitivity of the noise reduction to various parameters.

ACKNOWLEDGMENTS

This work was performed under the auspices of the U.S. Department of Energy by University of California Lawrence Livermore National Laboratory under contract No. W-7405-Eng-48.

REFERENCES

1. S. Weeratunga and C. Kamath, "PDE-based non-linear diffusion techniques for denoising scientific and industrial images: an empirical study," in *Proceedings, Image Processing:Algorithms and Systems, SPIE Electronic Imaging*, **4667**, pp. 279–290, 2002.
2. P. Perona and J. Malik, "Scale-space and edge detection using anisotropic diffusion," in *Proceedings, IEEE Computer Society workshop on Computer Vision*, pp. 16–27, 1987.
3. P. Perona and J. Malik, "Scale-space and edge detection using anisotropic diffusion," *IEEE Transactions on Pattern Analysis and Machine Intelligence* **12**(7), pp. 629–639, 1990.
4. J. Weickert, *Anisotropic diffusion in Image Processing*, B.G. Teubner, 1998.
5. E. B. Dam, "Evaluation of diffusion schemes for multi-scale watershed segmentation," Master's thesis, University of Copenhagen, Denmark, May 2000.
6. V. Vemuri and W. J. Karplus, *Digital Computer Treatment of Partial Differential Equations*, Prentice Hall, 1981.
7. J. Weickert and H. Scharr, "A scheme for coherence-enhancing diffusion filtering with optimized rotation invariance," *Journal of Visual Communication and Image Representation* **13**, pp. 103–118, 2002.
8. C. Tomasi and R. Manduchi, "Bilateral filtering for gray and color images," in *Proceedings, IEEE International Conference on Computer Vision*, pp. 839–846, 1998.
9. M. Elad, "On the origin of the bilateral filter and ways to improve it," *IEEE Transactions on Image Processing* **11**(10), pp. 1141–1151, 2002.
10. D. Barash, "Bilateral filtering and anisotropic diffusion: towards a unified viewpoint," technical report, hpl-2000-18 (r.1), Hewlett-Packard Laboratories, Israel, 2000.
11. C. Chen and C. Wang, "A simple edge preserving filtering technique for constructing multi-resolution systems of images," *Pattern Recognition Letters* **20**, pp. 495–506, 1999.

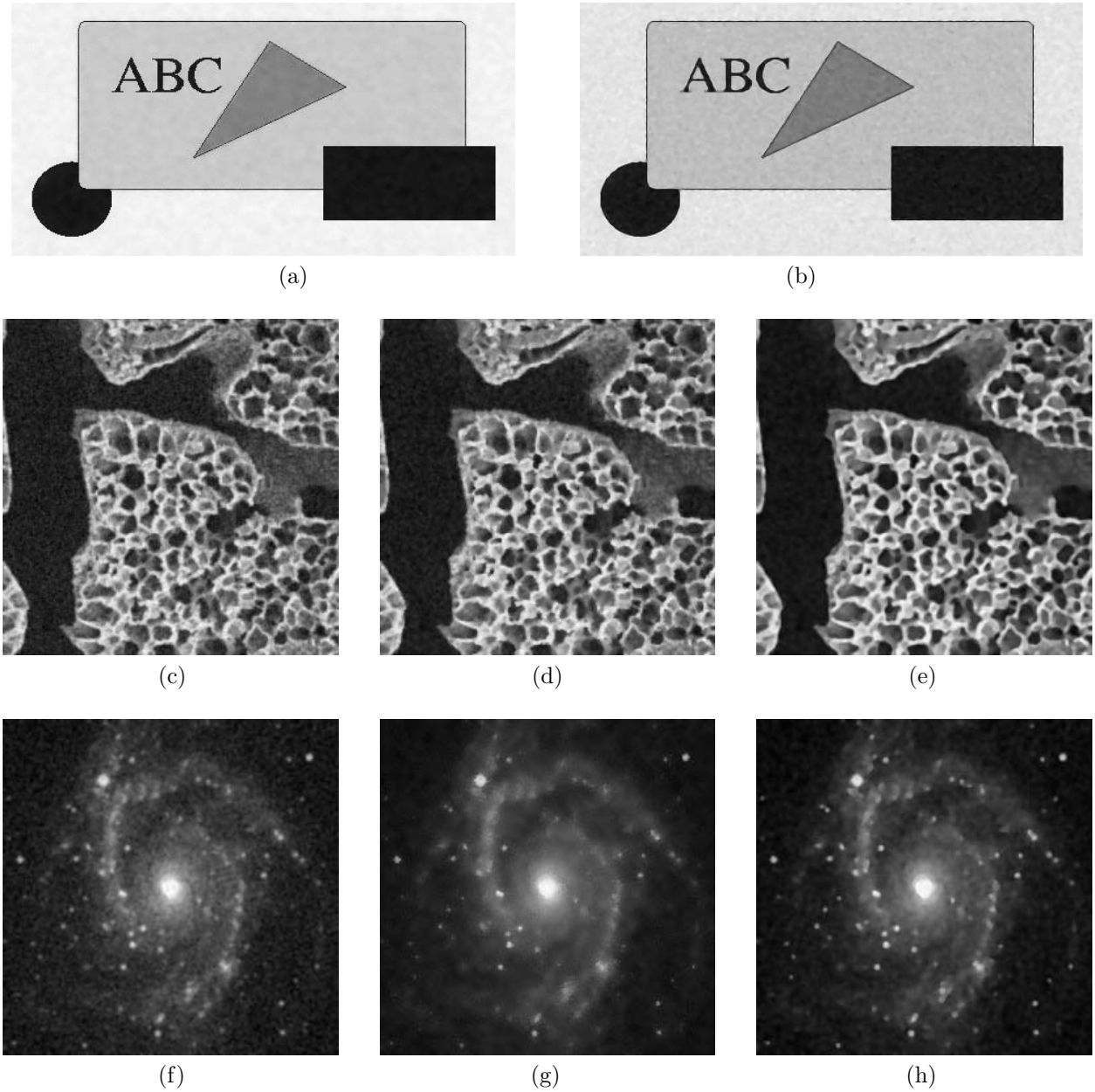

Figure 2. Denoised images: (a) Synthetic image, with Tomasi-Manduchi filter, MSE 28.7; (b) Synthetic image, with edge-enhancing anisotropic diffusion, MSE 71.9; (c) Lung image: best result with modified Chen-Wang filter, MSE=157.4; (d) Lung image: best result with Tomasi-Manduchi filter, MSE=151.2; (e) Lung image: best result with edge-enhancing anisotropic diffusion, MSE = 148.3; (f) Galaxy image: best result with modified Chen-Wang filter, MSE=57.7; (g) Galaxy image: best result with Tomasi-Manduchi filter, MSE=64.6; (h) Galaxy image: best result with edge-enhancing anisotropic diffusion, MSE = 39.0

Table 2. Lung image: Mean-squared error as a function of the four input parameters for the modified Chen-Wang filter. A pre-filter σ of 0.0 indicates that no pre-filtering is done. The MSE of the noisy image is 397.2.

Domain filter support	Domain filter σ	Pre-filter support	Pre-filter σ	MSE
4	2.0	2	0.5	219.8
3	2.0	2	0.5	190.6
2	2.0	2	0.5	162.9
2	1.0	2	0.5	157.4
2	0.5	2	0.5	249.6
2	1.0	1	0.5	168.6
2	1.0	1	0.25	352.5
2	1.0	1	0.75	161.3
2	1.0	1	1.0	176.2
2	1.0	1	1.5	190.8
2	1.0	1	0	337.1
4	1.0	1	0	336.4
4	2.0	1	0	275.4
4	3.0	1	0	263.6
4	4.0	1	0	263.7
4	10.0	1	0	269.1
5	1.0	1	0	336.4
5	2.0	1	0	274.7
5	3.0	1	0	265.1
6	5.0	1	0	286.9
7	5.0	1	0	295.9

Table 3. Galaxy image: Mean-squared error as a function of the four input parameters for the modified Chen-Wang filter. A pre-filter σ of 0.0 indicates that no pre-filtering is done. The MSE of the noisy image is 400.25.

Domain filter support	Domain filter σ	Pre-filter support	Pre-filter σ	MSE
4	2.0	2	0.5	90.2
3	2.0	2	0.5	89.9
2	2.0	2	0.5	90.9
2	1.0	2	0.5	109.2
2	0.5	2	0.5	232.8
2	1.0	1	0.5	109.3
2	1.0	1	0.25	320.1
2	1.0	1	0.75	65.7
2	1.0	1	1.0	59.3
2	1.0	1	1.5	57.7
2	1.0	1	0	323.1
4	1.0	1	0	321.9
4	2.0	1	0	228.2
4	3.0	1	0	195.8
4	4.0	1	0	184.8
4	10.0	1	0	174.4
5	1.0	1	0	321.9
5	2.0	1	0	226.1
5	3.0	1	0	190.1
6	5.0	1	0	171.1
7	5.0	1	0	170.2

Table 4. Test image 1: Mean-squared error as a function of the three input parameters for the Tomasi-Manduchi bilateral filter. The MSE of the noisy image is 401.16.

Filter support	Domain filter σ	Range filter σ	MSE
4	5.0	1.0	400.4
4	5.0	10.0	280.9
4	5.0	20.0	122.9
4	5.0	50.0	28.9
4	5.0	55.0	28.7
4	5.0	60.0	29.9
6	5.0	55.0	30.3
7	5.0	55.0	31.4
10	5.0	55.0	33.6
3	5.0	55.0	29.7
2	5.0	55.0	35.5

Table 5. Lung image: Mean-squared error as a function of the three input parameters for the Tomasi-Manduchi bilateral filter. The MSE of the noisy image is 397.2.

Filter support	Domain filter σ	Range filter σ	MSE
4	5.0	1.0	396.9
4	5.0	10.0	340.0
4	5.0	20.0	253.8
4	5.0	50.0	259.4
4	5.0	40.0	224.7
4	5.0	30.0	218.5
6	5.0	30.0	228.8
7	5.0	30.0	231.8
10	5.0	30.0	235.7
3	5.0	30.0	210.9
2	5.0	30.0	202.0
12	1	40.0	173.7
2	1	60.0	151.2

Table 6. Galaxy image: Mean-squared error as a function of the three input parameters for the Tomasi-Manduchi bilateral filter. The MSE of the noisy image is 400.25.

Filter support	Domain filter σ	Range filter σ	MSE
4	5.0	1.0	399.6
4	5.0	10.0	290.9
4	5.0	20.0	142.9
4	5.0	50.0	64.6
4	5.0	40.0	65.2
4	5.0	30.0	81.7
6	5.0	30.0	85.6
7	5.0	30.0	87.2
10	5.0	30.0	90.1
3	5.0	30.0	80.5
2	5.0	30.0	84.4
12	1.0	30.0	122.9

Table 7. Test image 1: Mean squared error as a function of the diffusivity perpendicular to the edge using the edge-enhancing anisotropic diffusion. See the text for the remainder of the parameters. The conductance K is for each of the diffusivity functions. The MSE of the noisy image is 401.16.

	Diffusivity functions					
Discretization, K	Perona-Malik (1)	Perona-Malik (2)	Charbonnier	Weickert (m=2)	Weickert (m=3)	Weickert (m=4)
Standard discretization, K=2.0	181.5	188.1	171.0	182.4	191.5	196.2
Standard discretization, K=5.0	151.9	139.7	200.2	133.8	134.1	135.6
Standard discretization, K=10.0	181.4	172.5	266.2	186.7	167.7	155.4
Standard discretization, K=15.0	228.7	230.3	309.8	272.3	266.7	261.9
Weickert non-negativity, K=2.0	98.7	104.5	106.8	101.5	108.8	112.8
Weickert non-negativity, K=5.0	89.5	76.5	155.8	73.6	71.9	72.3
Weickert non-negativity, K=10.0	133.1	121.1	236.3	138.1	116.5	102.9
Weickert non-negativity, K=15.0	189.5	187.7	288.2	233.4	224.1	217.6

Table 8. Lung image: Mean squared error as a function of the diffusivity perpendicular to the edge using the edge-enhancing anisotropic diffusion. See the text for the remainder of the parameters. The conductance K is for each of the diffusivity functions. The MSE of the noisy image is 397.2.

	Diffusivity functions					
Discretization, K	Perona-Malik (1)	Perona-Malik (2)	Charbonnier	Weickert (m=2)	Weickert (m=3)	Weickert (m=4)
Standard discretization, K=10.0	266.9	268.9	276.9	265.3	271.6	275.4
Standard discretization, K=15.0	263.1	258.0	299.8	259.8	258.9	260.3
Weickert non-negativity, K=10.0	152.8	148.8	207.4	154.2	150.1	148.3
Weickert non-negativity, K=15.0	176.4	172.6	252.4	187.5	176.5	170.9

Table 9. Galaxy image: Mean squared error as a function of the diffusivity perpendicular to the edge using the edge-enhancing anisotropic diffusion. See the text for the remainder of the parameters. The conductance K is for each of the diffusivity functions. The MSE of the noisy image is 400.25.

	Diffusivity functions					
Discretization, K	Perona-Malik (1)	Perona-Malik (2)	Charbonnier	Weickert (m=2)	Weickert (m=3)	Weickert (m=4)
Standard discretization, K=10.0	52.7	51.1	50.3	49.1	49.7	50.4
Standard discretization, K=15.0	49.9	49.2	50.5	49.6	49.3	49.1
Weickert non-negativity, K=10.0	40.2	39.5	43.7	39.9	39.3	39.0
Weickert non-negativity, K=15.0	42.0	42.7	46.8	45.4	44.4	43.7

University of California
Lawrence Livermore National Laboratory
Technical Information Department
Livermore, CA 94551